A98-31651

ICAS-98-5,8,1

CHARACTERISTICS OF MOMENTUM-DOMINATED HYDROCARBON TURBULENT DIFFUSION FLAMES*

U. Hegde and Z. G. Yuan
National Center for Microgravity Research, Cleveland, Ohio, U. S. A.
D. P. Stocker, NASA Lewis Research Center, Cleveland, Ohio, U. S. A.
M. Y. Bahadori, Science and Technology Development Corp., Los Angeles, U. S. A.

Abstract

This paper presents results obtained in a study of turbulent propane and methane gas-jet diffusion flames under momentum-dominated conditions in a microgravity environment. Experiments were conducted at the 2.2-Second Drop Tower and 5.18-Second Zero-Gravity Facility at NASA Lewis. These were supported by numerical modeling of the flame utilizing a k-ε formalism. Although momentum-dominated flames are important in practical applications such as jet and rocket engines, ramjets and other combustors, there is lack of information on these flames because, under normal gravity conditions, the high Froude numbers required also result in high Reynolds numbers. For hydrocarbon flames, this requirement leads to large flame sizes and intense turbulent conditions which are not practical to resolve. In the microgravity studies described here, momentum-dominated turbulent flames are obtained at moderate Reynolds numbers below 10000. Experiments to date have studied flame sizes, and temperature and pressure fluctuations. Findings described include (i) the larger size of the microgravity flames compared with their buoyancy-influenced normal-gravity counterparts , (ii) the presence of relatively higher frequency components in the normal gravity spectra compared to the microgravity case and (iii) computations which show that the axial velocity in the downstream regions of the normal-gravity flame can be more than twice those in the microgravity flame due to buoyant acceleration. The implications of these findings regarding the turbulence characteristics of the flames are discussed.

Introduction

Many flames in industry and nature are diffusion flames, i.e., flames in which the fuel and oxidizer are initially separate or non-premixed. Aerospace examples include flames in jet engines, gas turbine combustors, ramjets and rocket motors. Other industrial examples include flames in furnaces and boilers while forest fires are an important example of diffusion flames in nature. Because of their importance, diffusion flames represent a class of widely studied combustion phenomena. A fundamental basis for analyzing these flames was provided by Burke and Schumann[1] who argued that the location of the flame must coincide with the stoichiometric surface for fuel and oxidizer. Following this work, pioneering investigations of the behavior of turbulent diffusion flames were made by Hottel and Hawthorne[2] and Wohl et al[3] .

Primary avenues of research in turbulent diffusion flames focus on (a) dependence of global flame quantities such as flame height and flame shape on the flow conditions (i.e., fuel flow rate, nozzle size etc) and (b) the

* Submitted for presentation at the 21st ICAS Congress.

21st ICAS Congress
13-18 September 1998
Melbourne, Australia

behavior of the turbulent fluctuations in the flow field quantities such as temperature and velocity. Studies of type (a) are useful in estimating heat transfer rates and flame size whereas studies of type (b) are useful for validating flame models, gaining insight into the flame structure, and exploring avenues for flame control.

Apart from the geometry of the combustor, the momentum of the fuel (and/or air) jet is important in classifying the flame behavior. In general, gas-jet diffusion flames may be classified as momentum-dominated, buoyancy-dominated or flames that are influenced by both momentum and buoyancy. Similitude and scaling arguments have been presented in the literature (for example, Blake and McDonald[4]) to distinguish these regimes based upon density-weighted Froude and Richardson numbers. Based on these arguments, in the buoyancy-dominated regime, the non-dimensional flame height, L_f, increases with the weighted Froude number, F, as

$$L_f = 6\,F^{0.2}$$

whereas in the momentum-dominated regime it asymptotes to a value given by

$$L_f = 11$$

For intermediate values of F, both buoyancy and jet momentum effects are important.

It is to be noted that momentum-dominated flames have been reportedly achieved in laboratories only for hydrogen and carbon monoxide gas-jet flames. The primary reason that momentum-dominated flames for other fuels have not been investigated appears to be that at large Froude numbers, the flame lengths become much larger than what can be practically studied. Furthermore, to obtain momentum-dominated flames under normal-gravity conditions requires extremely high jet velocities of the order of tens of meters/second which leads to extremely large Reynolds number for typical nozzle sizes used in the laboratory. This, in turn, leads to problems in resolving the turbulent flow field both experimentally and computationally. Thus, there is a lack of information about momentum-dominated flame characteristics for hydrocarbon flames. However, most practical fuels used in industry are hydrocarbon based. Thus, there is a need to extend the momentum-dominated flame studies to hydrocarbon flames.

In microgravity, momentum-dominated turbulent flames are obtained at much smaller velocities than in normal gravity. Thus, significantly larger length and time microscales of the turbulent flow field under momentum-dominated conditions are obtained. Hence, studying and making measurements in turbulent gas-jet diffusion flames in microgravity offers the potential to capture the details of the turbulent flow field under momentum-dominated conditions.

The first investigations on hydrocarbon turbulent diffusion flames in microgravity were initiated recently[5]. These studies have shown that significant differences exist in the transition processes in normal-gravity and microgravity flames, and that the turbulent flames in microgravity behave very differently as compared to their buoyancy-dominated normal-gravity counterparts[6]. For example, in the transition regime while the visible flame height, for given fuel and nozzle size, in normal gravity decreases, the height of the microgravity flame increases . In the fully developed turbulent regime, the normal-gravity flame height is independent of injection velocity, whereas the microgravity flame height continues to increase, although at a lower rate than in the laminar and transitional regimes. Other differences between the normal-gravity and microgravity flames arise in the jet shear-layer instability characteristics, extent of the transitional regime and blow-off limit characteristics[7].

The primary reason that these differences exist between buoyancy-dominated and momentum dominated flames is because of differences in flow pattern caused by buoyant flow acceleration and entrainment. For example, buoyant acceleration counteracts the centerline velocity decay that would otherwise occur due to jet spreading and momentum diffusion. That such flow differences yield different flame characteristics may be explained by noting that the primary time scales in diffusion flames have components of flow time and chemical time. Flow time scales are related to flow processes such as mixing of fuel and oxidizer prior to reaction whereas chemical time scales are related to the times for the various reactions occurring in the flame. In most cases, flow times are several orders of magnitude larger than chemical times, with the result that flow processes control characteristics of diffusion flames such as size and shape. Hence, factors such as buoyancy that modify the flow patterns in these flames are expected to have significant influence on flame behavior.

This paper provides descriptions of both global time-averaged flame quantities such as flame size as well as results on the turbulence structure of momentum-dominated hydrocarbon flames in microgravity. The global flame features are compared with predictions from a numerical procedure utilizing the standard k-ε turbulence model. Temperature and pressure spectra from the flames are described and differences with the normal-gravity case are presented. The experimental apparatus is described in the next section. This is followed by a brief outline of the numerical model. The Results and Discussion section then follows.

Experimental Apparatus

Most of the the microgravity experiments in this study were conducted at the 5.18-Second Zero-Gravity Facility at NASA Lewis. Some tests on the flame height were conducted at the 2.2 Second Drop Tower at NASA Lewis. The Zero-Gravity Facility consists of a 6.1-m diameter steel-walled vacuum chamber that provides a 132-m free fall distance. Prior to each test, the chamber is evacuated to a pressure of about 1 Pa to eliminate air drag. The drop is initiated by shearing a bolt that suspends the experiment vessel assembly. This assembly then falls in the chamber and is decelerated at the bottom by impact into a 6.1-m deep container filled with expanded polystyrene pellets. More information on this facility and the 2.2 Second Drop Tower may be found elsewhere[8].

The experiment vessel is a cylindrical chamber approximately 80 liters in volume with a length of about 50 cm. Fuel-nitrogen mixtures are injected into quiescent air through a nozzle made of stainless steel tubing. For the tests to be described, methane and propane were used as fuel. The flame is ignited just after the drop commences by means of a hot wire mounted on a rotary actuator which retracts the igniter out of the flow field after ignition.

Side views of the flame are imaged by means of video cameras at 30 frames per second. Type K thermocouples with bead diameters in the range of 150-200 microns are strung across the flame at various axial locations above the nozzle tip. To date, temperature measurements in the lower half of the flame have been made and will be described. The measured signals from the thermocouples have to be compensated for their time response in order to measure the temperature spectrum. The technique for obtaining the time constant has been described before[9]. The acoustic pressure generated by the flames have been measured utilizing a condenser microphone assembly mounted near the chamber side wall. The microphone has a flat frequency response to about 10,000 Hz. A 16-bit data acquisition

system is utilized for the temperature and pressure measurements. Sampling rates for the thermocouples are 1000 Hz while the pressure measurements are sampled at up to 5000 Hz

Computational Model

The numerical model utilizes standard turbulent models in conjunction with state relationships for chemistry for predicting the time-averaged flow field . Thus, the set of governing equations utilized are of the form

$$\mathrm{div}(\rho u\phi - \Gamma_\phi \mathrm{grad}\phi) = S_\phi$$

where

$\phi = u, v, w$: Momentum

$\Gamma_\phi = \rho (\nu_t + \nu_l)$

S_ϕ = -grad(p) + gravity + viscous

$\phi = h$: Enthalpy

$\Gamma_\phi = \rho (\nu_t + \nu_l)/ \sigma_h$

S_ϕ = -Dp/Dt + heat sources

$\phi = 1$: Continuity

$\Gamma_\phi = 0$

S_ϕ = mass sources

In the above equations, u, v, and w are the three components of the velocity, ρ is density, p is pressure, h is enthalpy, and ν_t and ν_l are the turbulent and laminar kinematic viscosities, respectively. These equations are supplemented by equations for the turbulent kinetic energy, k, and the dissipation rate, ε. The model solves for pressure, velocity, temperatures, species concentrations, and turbulent kinetic energy and dissipation rate. The code utilizes a discrete transfer radiation model[10] for CO2 and H2O emissions for radiative transport.

Results and Discussion

A. Time-averaged Flame Properties

(i) Flame Height

Fig. 1 plots measured flame heights for propane flames burning in quiescent air under normal gravity and microgravity conditions as a function of injection Reynolds number. Nozzle diameter for these tests was 0.8 mm. The laminar-to- turbulent transition regime for these flames is approximately between Reynolds numbers of 2000 and 3000. It is seen that the microgravity flames are much taller than their normal gravity counterparts as noted earlier. It is also found that the turbulent microgravity flames exhibit closed tips in contrast to the microgravity laminar propanr flames which have open tips[5].

In the model predictions, the flame height is obtained from considerations of the centerline axial profiles of fuel and oxidizer. The computed mass fraction profiles are shown for two nozzle diameters for zero-gravity conditions in Fig. 2. In this case, the injection Reynolds number is 5000 for both cases. The flow rate for the smaller (0.8 mm) diameter nozzle is therefore half that of the larger (1.6 mm) diameter nozzle case. There are different ways in which the flame height can be defined, for example, the location where fuel and oxidizer are in stoichiometric proportions or the fuel concentration becomes vanishingly small. They all yield similar results. For example, taking the location where the fuel concentration becomes very small (mass fraction< 0.001 for specificity) , the computed average flame height for the 1.6 mm dia nozzle is 30 cm whereas that for the 0.8 mm dia nozzle is around 15 cm. This dependence

of flame height on flow rate and nozzle diameter is well known for normal-gravity flames and is verified here for the microgravity case. However, the model underpredicts the observed flame length in microgravity by a factor of approximately two.

Next, consider the relative flame height predictions for corresponding zero gravity and normal gravity flames. The axial mass fraction profiles are shown in Fig. 3 for the 1.6 mm diameter nozzle case for injection Reynolds number of 5000. It is seen that the normal- gravity flame height is predicted to be around 26 cm. This is found to agree reasonably well with the experimental result. However, as noted , the zero-gravity flame height is underpredicted by the model.

(ii) Temperature and Velocity

Figure 3 also plots the axial profile of the computed time-averaged temperature. The peak temperature is predicted to occur somewhat upstream of the flame tip as defined. In addition, the peak temperature for the zero-gravity case is lower than the normal gravity case. As with laminar diffusion flames, the lower values of peak temperature in microgravity are believed to be due to higher radiative loss[11]. In normal gravity, the velocities near the tip are higher (see Fig. 4) and indicate that a larger fraction of heat is lost by convection as the hot combustion gases move out of the domain. In microgravity, with the smaller velocities, the hot gases remain in the flame domain longer and lose additional heat by radiation during this time. This results in a lowering of the temperature in the domain. This behavior was verified by removing the radiative loss in the computations. The peak temperatures were then found to be same for both the microgravity and normal-gravity flames.

Computations show that for both the normal gravity and microgravity cases, at the injection velocities considered (on the order of 10 m/sec), the axial velocity along the flame centerline exhibits a decay. However, for the normal-gravity case the velocity decay is lower than for the microgravity case. This is shown in Fig. 4 which plots the ratio of the axial velocity for the normal-gravity case to that for the zero gravity case as a function of axial distance from the nozzle exit. It is seen that in the downstream regions of the flame, the axial velocity for the normal-gravity case can be more than twice that in the microgravity case.

B. Turbulence Characteristics

(i) Implications of time-averaged results

As noted, the microgravity turbulent flames are observed to be taller (see Fig. 1) at the moderate injection Reynolds numbers of interest. Utilizing the argument of the equality between the characteristic time for diffusion and the travel time from the nozzle exit to the flame tip[12], it was shown[6] that the effective (or turbulent) diffusivity of the normal-gravity flame was two to three times that of the microgravity flame at the moderate Reynolds numbers studied (less than 10,000 based upon jet injection velocity and cold fuel properties). Two reasons for this difference are forwarded, both of which arise from the local centerline velocity in the flame being greater for the normal gravity case due to buoyant acceleration. The turbulent diffusivity will scale with the velocity which is larger for the normal gravity case. Second, the spectrum of turbulence for the normal-gravity flame is expected to extend to smaller scales as compared to the microgravity case where the velocity decay is greater. This follows from turbulence dissipation behavior which scales with u'/l where u' is the turbulent velocity fluctuation magnitude and l is the integral length scale[13]. This is a measure of the highest frequencies (i.e., the smallest scales) in the turbulent spectrum. The integral length scale is

expected to be relatively invariant over the flame length and being of the order of the nozzle diameter is similar for both the normal gravity and microgravity cases whereas u' will scale with the mean velocity which is greater for the normal gravity case. Based upon the ratio of the axial velocities (Fig. 4) the turbulent spectrum may be expected to be twice as broad in frequency range in the normal gravity case. Supporting experimental evidence is provided in the next section. Smaller scales promote local mixing thereby increasing the effective diffusivity of fuel and oxidizer at the flame which results in flame shortening.

(ii) Pressure Spectra

Pressure spectra of the acoustic field radiated from the flames have also been obtained. The radiated sound field is related to the time-dependent volumetric heat release rate of the flame[14]. In the absence of chamber resonant excitation, the frequency content of the pressure spectrum provides a good estimate of the frequency content of the fluctuations in the flame region and an estimate of the turbulent spectrum frequency bandwidth.

Figures 5 and 6 plot measured pressure spectra of a normal gravity and the corresponding microgravity methane flame, respectively. The injection Reynolds number is about 2000. The pressure measurements were made near the chamber side wall at the same physical location. The flame size in the normal and microgravity cases are quite different so that a comparison of the amplitudes is not straightforward. However, no chamber resonant frequency effects are observed in the two spectra suggesting that the frequency range of the spectra are indicative of the corresponding frequency range of the flame region fluctuations. It is observed that the frequency above which structure in the microgravity spectrum vanishes is between 80 -100 Hz (as evidenced by cessation of ripples in the spectrum). However, for the normal gravity case, structure exists in the spectrum out to about 200 Hz.

The above finding is consistent with the idea stated above that the turbulence spectrum for the normal gravity case will extend to smaller scales (i.e., higher frequencies) as compared to the corresponding microgravity flame. It is also consistent with increased effective diffusivity in the normal-gravity flame.

(iii) Temperature Spectra and Cross spectra

Thermocouple measurements have been utilized to measure temperature on the flame centerline and obtain the corresponding spectra. Figure 7 shows the measured temperature at non-dimensional heights of x/d = 9 and 70 , respectively. Figure 8 shows the obtained spectra. These locations are in the lower half of the flame. The zero frequency component has been removed in each case. In addition, these spectra have been truncated at frequencies above which the signal to noise ratio was judged to be unsatisfactory; however, in both cases the spectral levels have dropped by about 10 dB from their highest levels at this point.

These spectra show that at the downstream location (x/d = 70) the temperature fluctuations have higher amplitudes with spectral levels about 10-15 dB greater than at the lower level (x/d = 9). In addition, the fall off in spectral level with frequency is steeper at the lower location. This indicates that the flame becomes more turbulent with increasing axial distance in the lower half of the flame.

The magnitude of the cross spectrum of the temperature fluctuations at the two locations is shown in Fig. 9. The fall off in amplitude with frequency is similar to the

autospectrum at the lower location indicating that the fluctuations at the higher location are only weakly correlated to those at the lower location.

Figure 10 plots the autocorrelation coefficient of the temperature signals at the two axial locations. The fall off with time lag is steeper at the downstream location indicating a smaller time scale over which the oscillations are correlated. This is consistent with the spectral results (Fig. 8) which show that the flame is more turbulent here.

It is of interest to determine whether the flame will continue to become more turbulent in the upper half of the flame or whether the spectrum will begin to decay further downstream. It is expected, based upon the velocity decay in the downstream regions of the flame that the spectrum will begin to decay both in amplitude of the broadband region as well as in the range of frequencies. This will be returned to in future work.

Conclusions

Experimental and modeling results on momentum-dominated hydrocarbon turbulent gas-jet diffusion flames in microgravity have been presented in this paper. The microgravity environment provided the means to suppress the effects of buoyancy even at moderate injection velocities. Findings include:

(a) the microgravity flames are significantly larger than their normal gravity counterparts
(b) the flow velocity in the downstream regions of the flame in the normal gravity case can be more than twice that in the microgravity case due to buoyant acceleration
(c) the mean temperatures in the microgravity flame are lower than those in the normal gravity flame which is believed to be due to increased radiative loss in microgravity
(d) the spectra of the radiated pressure field shows that the spectra of the buoyancy-influenced normal gravity flame extends to more than twice the frequency of the microgravity case; this suggests an increased effective diffusivity for the normal gravity flame and is consistent with the larger flame sizes in microgravity
(e) temperature spectra from the lower half of the microgravity flame indicate that turbulence levels increase with axial distance; however, it is expected that further downstream the turbulence will decay.

Acknowledgments

This work was supported by NASA Lewis Research Center. The assistance of Dennis Thompson, Zero-G Facility manager, in the conduct of the tests is greatly appreciated. Jonathan Sakai of the University of Dayton assisted with the numerical code computations during an internship at NASA Lewis.

References

1. Burke, S. P., and Schumann, T. E. W. (1928). *Ind. Eng. Chem.*, vol. 20, p.988.
2. Hottel, H. C., and Hawthorne, W. R. (1949). Diffusion in Laminar Flame Jets. *Third Symposium on Combustion*, Williams and Wilkins Co., Baltimore, p. 254.
3. Wohl, K., Gazley, C., and Kapp, N. (1949). Diffusion Flames. *Third Symposium on Combustion*, Williams and Wilkins Co., Baltimore, p. 288.
4. Blake, T. R. and McDonald, M. [1995] *Combustion and Flame*, vol. 101, pp. 175-184.
5. Bahadori, M. Y., Stocker, D. P., Vaughan, D. F., Zhou, L., and Edelman, R. B. (1993). Effects of Buoyancy on Laminar, Transitional and Turbulent Gas Jet Diffusion Flames. In Williams, F. A., Oppenheim, A. K., Olfe, D. B., and Lapp, M. (Eds.), *Modern Developments in Energy, Combustion and Spectroscopy*, Pergamon Press, pp. 49-66.
6. Hegde, U., Zhou, L., and Bahadori, M. Y. (1994) *Combustion Science and Technology*, vol. 102, pp. 95-113.
7. Zhou, L., Hegde, U., and Bahadori, M. Y. (1993) Experimental Observations of Turbulent Gas Jet Diffusion Flames in Microgravity. Joint Central and Eastern States Section Meeting of the Combustion Institute, New Orleans, Louisiana.
8. NASA (1995) *TM 106858*, Lewis Research Center.
9. Hegde, U., Stocker, D. P., and Bahadori, M. Y. (1996) AIAA Paper No. 96-0621.

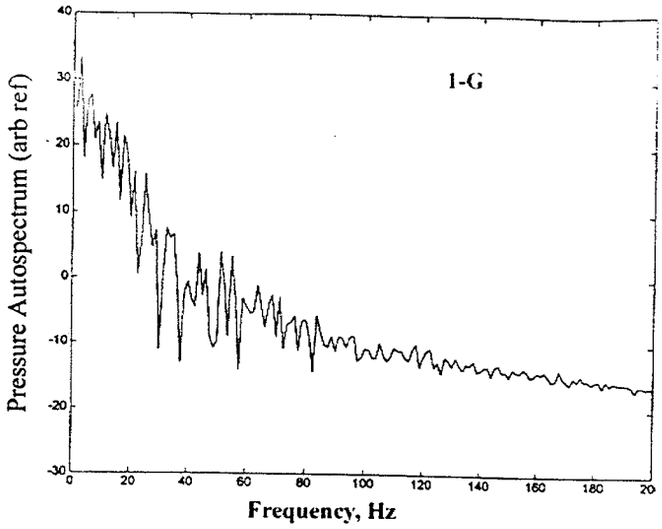

Fig. 5 Acoustic pressure spectrum of a normal-gravity methane-air gas-jet diffusion flame. Nozzle i.d. is 1.6 mm and injection Reynolds number is approximately 2000.

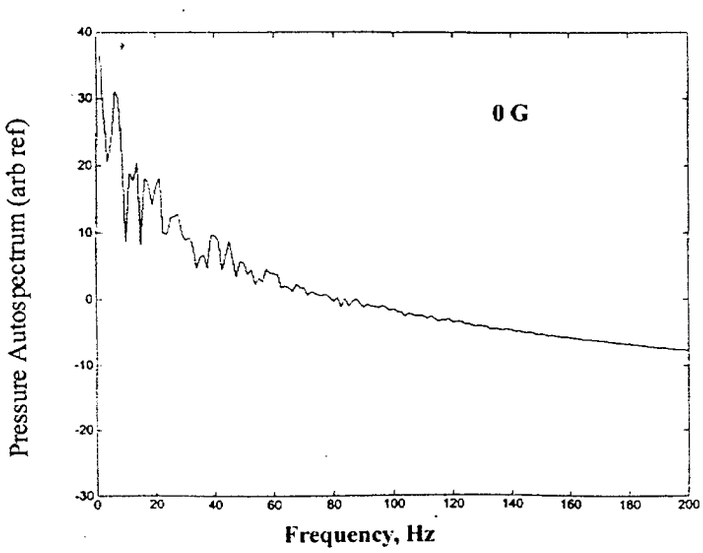

Fig. 6 Acoustic pressure spectrum of a micro gravity methane-air gas-jet diffusion flame. Nozzle i.d. is 1.6 mm and injection Reynolds number is approximately 2000.

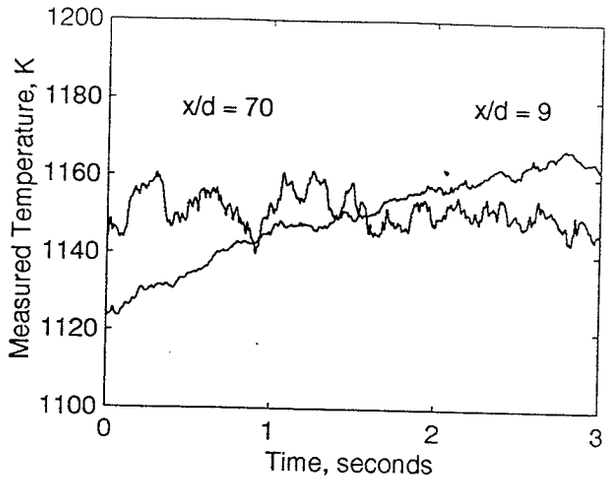

Fig. 7 Measured centerline temperatures at two axial locations. Fuel jet of 60% propane and 40% nitrogen injected into quiescent air in microgravity. Injection Reynolds number is 2600.

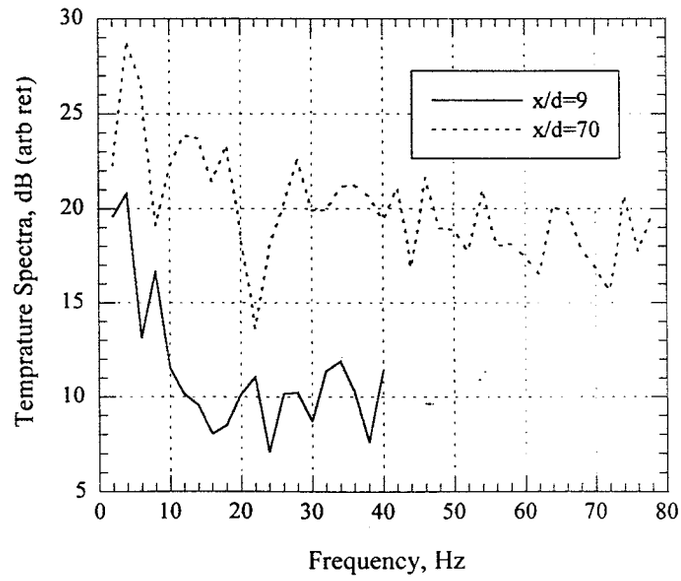

Fig. 8 Centerline temperature spectra at two axial locations. Flame conditions as in Fig. 7

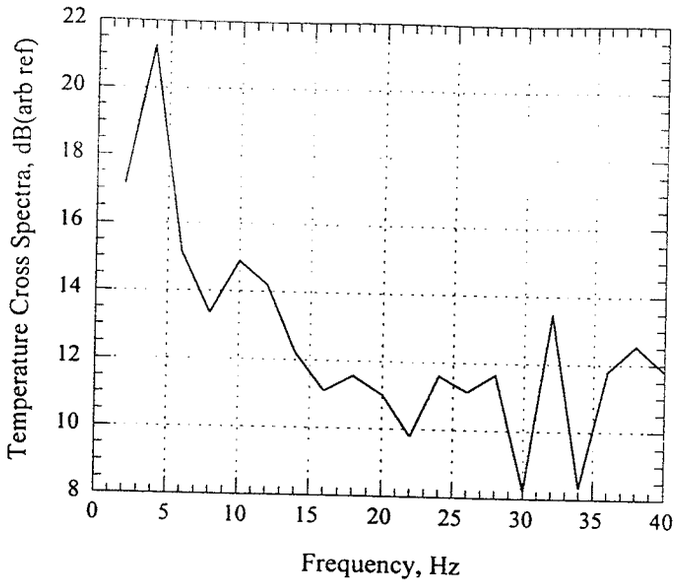

Fig. 9 Temperature cross spectrum between axially separated centerline locations of x/d = 9 and x/d =70. Flame conditions as in Fig. 7.

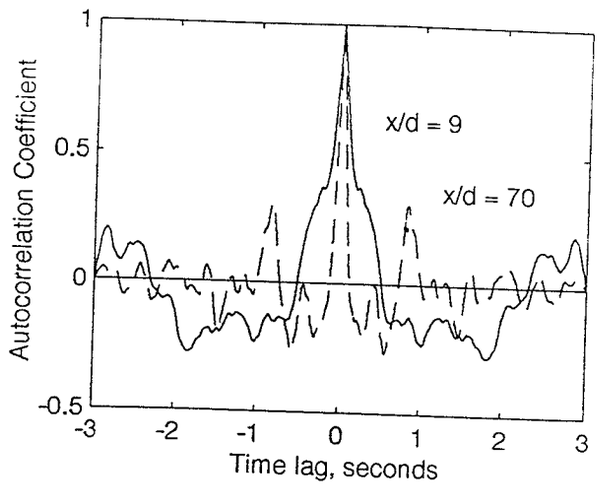

Fig. 10 Autocorrelations of temperature at axially separated centerline locations of x/d = 9 and x/d = 70. Flame conditions as in Fig. 7.